Crystal structure and ferroelectric properties of ϵ-Ga2O3 films grown on (0001)-sapphire

Inorganic Chemistry

Article

pubs.acs.org/IC

Crystal Structure and Ferroelectric Properties of ε-Ga_2O_3 Films Grown on (0001)-Sapphire

Francesco Mezzadri,*[,†,‡] Gianluca Calestani,[†] Francesco Boschi,[‡,§] Davide Delmonte,[‡] Matteo Bosi,[‡] and Roberto Fornari[‡,§]

[†]Department of Chemistry, University of Parma, Parco Area delle Scienze 17/A 43124 Parma, Italy

[‡]IMEM-CNR, Parco Area delle Scienze 37/A, 43124 Parma, Italy

[§]Department of Physics and Earth Sciences, University of Parma, Parco Area delle Scienze 7/A, 43124 Parma, Italy

Supporting Information

ABSTRACT: The crystal structure and ferroelectric properties of ε-Ga_2O_3 deposited by low-temperature MOCVD on (0001)-sapphire were investigated by single-crystal X-ray diffraction and the dynamic hysteresis measurement technique. A thorough investigation of this relatively unknown polymorph of Ga_2O_3 showed that it is composed of layers of both octahedrally and tetrahedrally coordinated Ga^{3+} sites, which appear to be occupied with a 66% probability. The refinement of the crystal structure in the noncentrosymmetric space group $P6_3mc$ pointed out the presence of uncompensated electrical dipoles suggesting ferroelectric properties, which were finally demonstrated by independent measurements of the ferroelectric hysteresis. A clear epitaxial relation is observed with respect to the *c*-oriented sapphire substrate, with the Ga_2O_3 [10−10] direction being parallel to the Al_2O_3 direction [11−20], yielding a lattice mismatch of about 4.1%.

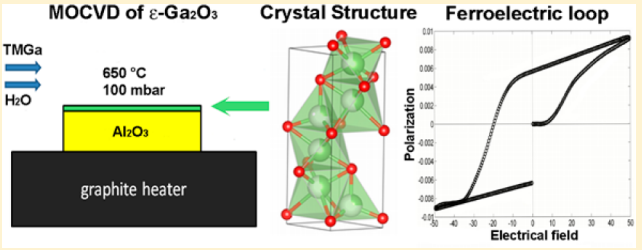

INTRODUCTION

Gallium oxide (Ga_2O_3) is a well-known sesquioxide with semiconducting properties. It may present five different polymorphs, α, β, γ, δ, and ε, each with different structure and physical properties. In the past few years, most research and technological development have focused on β-Ga_2O_3, especially because large single crystals[1−3] and oriented substrates of this material were made available for epitaxy. These technological developments led to deposition of high-quality homoepitaxial films of β-Ga_2O_3[4−6] and to fabrication of novel devices for high-power electronics[7] and UV detection.[8] Although the major attention is still focused on the β polymorph, there has been an increasing parallel interest also on the other phases, beginning from the pioneering work by Roy et al., who provided the first unambiguous identification of the different polymorphs in 1952.[9] Among the polymorphs, the ε phase is particularly interesting because of its higher symmetry and simpler epitaxial growth conditions with respect to the more popular β phase. Furthermore, it shows a favorable matching to commercial sapphire as well as to other hexagonal or pseudohexagonal substrates.[10−12] Recently, there were theoretical studies aiming at establishing structure and formation energy, i.e. thermodynamic stability, of the different polymorphs.[13] While these first-principles calculations were able to give a qualitative description of the formation energies, concluding that the β phase (monoclinic phase) is the most stable polymorph, they failed in reproducing the actual structure of the ε phase. Some theoretical papers[13,14] suggested that this polymorph is orthorhombic, while recent experimental studies concur that it is hexagonal.[10−12,15] Although theoretical estimates and experimental observations indicate that ε-Ga_2O_3 is metastable, it was recently observed that this phase remains stable up to at least 650 °C and that only after prolonged annealing at T > 800 °C does it undergo a complete transition to β.[10−12] This allows sufficiently high working temperatures for devices based on ε-Ga_2O_3, which makes this phase very interesting in view of practical applications and justifies further investigations. Providing new information and enriching the very limited body of knowledge on ε-Ga_2O_3 is exactly the motivation of the present work. Here, the main aim is to provide a precise description of crystal structure and lattice parameters. Actually, in the literature we just found one report[15] regarding a structure determination of the ε phase by neutron diffraction. In that report, ε-Ga_2O_3 was prepared via thermal decomposition of gallium nitrate, which unfortunately never supplied phase-pure materials but rather a mixture of β- and ε-Ga_2O_3. Nevertheless, the authors succeeded in solving the structure of the ε phase, albeit possibly distorted by the β contamination. They suggested that this polymorph was constituted by an hexagonal close-packed array of oxygen ions with partial filling of octahedral and tetrahedral sites. In the present work, single-crystal diffraction of phase-pure ε-Ga_2O_3 provides an accurate description of the structure of this material

Received: September 16, 2016

DOI: 10.1021/acs.inorgchem.6b02244
Inorg. Chem. XXXX, XXX, XXX−XXX

in thin film form, confirming from one side the results of ref 15 but showing that the positive and negative charges barycenters do not coincide. This gives rise to uncompensated electrical dipoles and to ferroelectric properties, as demonstrated by independent measurements of the ferroelectric hysteresis. Further, the epitaxial relations between the single-crystalline ε-Ga_2O_3 layer and the α-Al_2O_3 substrate were determined along with an estimate of their lattice mismatch.

EXPERIMENTAL SECTION

A thick ε-Ga_2O_3 layer (thickness of about 3 μm) was grown on *c*-plane sapphire by MOCVD (metal-organic chemical vapor deposition) at 650 °C and 100 mbar using water and trimethylgallium (TMG) as reagents and palladium-purified H_2 as carrier. The use of H_2O was observed to be more favorable, probably due to the higher reactivity of atomic oxygen from water dissociation with respect to molecular oxygen. The H_2O to TMG partial pressure ratio was varied in the range 100−1000 and generally set at 200. More details regarding the growth procedure can be found in ref 11. Under these growth conditions, all layers were reproducibly of ε phase. The precursor ratio and relatively low deposition temperature are in our opinion decisive factors in deciding what polymorph of Ga_2O_3 is actually grown. This would indicate that thermodynamics rather than kinetics plays the dominant role. This is supported by the experimental evidence that so far the ε phase has been reported in connection with HVPE and MOCVD growth experiments, but never as a result of deposition by pure kinetic methods such as MBE or PLD, although conducted at low temperature. Furthermore, it was demonstrated also recently[16] that MOCVD at temperature higher than 800 °C invariably leads to β-Ga_2O_3. While this can be easily understood remembering that β is the only thermodynamic stable polymorph, the failure in obtaining the ε phase by means of kinetic methods, even at low temperatures, probably lies in the higher distance from thermodynamic equilibrium of these methods: i.e., the very energetic species adsorbed at the substrate surface do not promote ε but just β nucleation. The sample was then properly prepared for single-crystal X-ray diffraction in order to maximize the diffraction intensities of the film with respect to those of sapphire. The substrate thickness was mechanically reduced with a lapping machine down to about 200 μm by using 60 grit sandpaper. The sample dimensions were then further reduced by mechanical cleavage, which allowed obtaining small fragments suitable for single-crystal diffraction experiments. X-ray diffraction (XRD) data were collected with Mo Kα radiation on a Bruker AXS Smart diffractometer, equipped with an APEX II CCD area detector. The reconstruction of precession images was carried out using the Precession Images plugin available in the Bruker APEX2 software. The ferroelectric properties were tested using the TF-Analyzer 2000E AixACcT system equipped with the Ferroelectric Module (FE-Module). The sample was previously metalized by sputtering 100 nm of gold on both surfaces of a rectangular specimen with surface area of 3.55 mm^2, in the so-called planar-plate capacitor configuration, and then annealing for 24 h at 100 °C. As a result the studied sample can be idealized as two capacitors in series: 200 μm thick Al_2O_3 and 3 μm thick ε-Ga_2O_3. The measurements were performed at room temperature, exploiting the dynamic hysteresis measurement (DHM) protocol (see the Supporting Information for more details about the method). An ac triangular bias between 0 and 1 kV, and frequency below 1500 Hz were applied. The current flowing through the dielectric was recorded as a function of the real-time value of the applied voltage during the triangular wave signal. In order to get the maximum contribution from the polar-induced current produced by ε-Ga_2O_3 and to reduce the relative weight of the displacement current promoted by sapphire, the current was collected from the gold plate on the film side. Blank measurements were performed also on a sapphire sample. The obtained data were analyzed using the Matlab platform.

RESULTS AND DISCUSSION

Single-crystal diffraction experiments, carried out on a 200 μm thick sample (film plus thinned substrate), as expected showed 2D diffraction patterns, constituted by the superimposition of two lattices. The first lattice was characterized by reflections with higher intensity, indexed in an hexagonal lattice with a = 4.759(1) Å and c = 12.992(3) Å and corresponding to the sapphire substrate,[17] while the weaker reflections could be indexed with a smaller hexagonal cell with a = 2.906(2) Å and c = 9.255(8) Å, corresponding to the Ga_2O_3 film. In Figure 1 a precession image reconstructed on the basis of the collected reciprocal space is reported, allowing identification of the relative orientation of the two lattices.

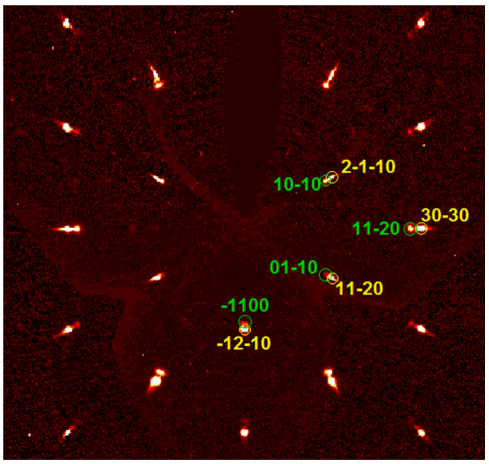

Figure 1. Precession image reconstructed by single-crystal diffraction data, *hki*0 projection; yellow and green labels refer to Al_2O_3 and Ga_2O_3 reflections, respectively.

As can be seen, despite the low thickness of the ε-Ga_2O_3 film, its excellent crystal quality gives rise to well-defined and relatively intense diffraction peaks. The *hki*0 plane shows the presence of two almost coincident hexagonal lattices with slightly different *d* spacings. No extra peaks or powder rings were detected, indicating the good quality of the film. The Ga_2O_3 [10−10] direction is aligned with the Al_2O_3 [11−20] direction, and consequently the two hexagonal lattices are rotated in the *ab* plane by 30° with respect to each other. On the other side, the difference in the *c* axes gives rise to a more complex pattern in the 1*kil* plane (see Figure S1 in the Supporting Information), where completely different reflection sequences are produced for the two phases. In order to obtain diffraction data suitable for quantitative structural analysis, a small fragment with approximate dimensions 193 × 64 × 16 μm^3 (the first number being the thickness of the film plus residual substrate) was used, which allows for a reduction of the intensity of the reflections from the substrate by several orders of magnitude. At the same time, by increasing the sample to detector distance from 50 to 70 mm, it was possible to isolate the diffraction spots of the Ga_2O_3 phase. In this way, the ε-Ga_2O_3 intensities could be accurately determined despite the stronger Al_2O_3 reflections, which in a first instance impeded the precise determination of the gallium oxide related intensities, in particular at low θ values. The presence of Al_2O_3 on one side of the sample, producing asymmetrical absorption, gives rise to large scale factor variations, in the 0.7−1.4 range, and unavoidably produces high residuals in merging reflections

DOI: 10.1021/acs.inorgchem.6b02244
Inorg. Chem. XXXX, XXX, XXX−XXX

Table 1. Selected Interatomic Distances, Formal Oxidation States ($Q(ij)$), Equivalent Coordination Numbers (ECoN), and Ion Charges

atoms	bond length (Å)	atoms	bond length (Å)	atoms	bond length (Å)	atoms	bond length (Å)
GA1−O1 (×3)	1.94(2)	GA2−O1 (×3)	1.944(18)	GA3−O2 (×3)	1.778 (10)	GA1−GA3	1.797(18)
GA1−O1 (×3)	2.072(15)	GA2−O2 (×3)	2.23(2)	GA3−O1	1.87(5)	GA1−GA2	1.947(15)
av	2.006(18)	av	2.087(19)	av	1.80 (2)	GA2−GA3	1.890(10)
$Q(ij)$	1.979	$Q(ij)$	1.011	$Q(ij)$	1.01		
ECoN	5.721	ECoN	4.811	ECoN	3.932		
$Q(ij)$/sof	2.968	$Q(ij)$/sof	2.889	$Q(ij)$/sof	3.176		

(R_{int} = 0.21%). Nonetheless, the quality of the data is not dramatically affected by absorption, allowing reliable structural solution and refinement, as discussed in the following. The Sir2011 suite was used for structure solution,[18] while refinement was carried out using the Shelxl software.[19] The cell parameters, refined by using the positions of 46 reflections in the theta range 4.401−19.914°, are a = 2.9081(7) and c = 9.262(3) Å. The analysis of the systematic absences, showing reflection conditions $hh\bar{2}hl = 2n$ and $000l = 2n$, is compatible with the $P6_3/mmc$, $P\bar{6}2c$, and $P6_3mc$ space groups. While the structure solution process failed in the first two cases, a plausible result was obtained for the $P6_3mc$ space group. It has to be noted that the found solution may look wrong at first sight, since it implies a close-packed layered model in which the ratio between cationic and anionic sites is reversed with respect to the expected value (3/2 instead of 2/3). However, the full-matrix refinement, carried out on 102 unique reflections, pointed out unusually large values of the atomic displacement parameters (adps) of the cations that can be interpreted as a fingerprint of the statistical occupation of gallium sites. When refined independently as free variables, the gallium site occupancies converged to values that are in good agreement with the expected Ga_2O_3 stoichiometry, leading to a normalization of the adps. In particular, the occupancy of the GA1 site, occupying an octahedral cavity between two adjacent close-packed layers of oxygens, converged to 2/3. The same happens when the global occupancy of GA2 and GA3, which occupy in mutually exclusive ways the octahedral and tetrahedral cavities between the next adjacent layers, are considered. Therefore, the site occupancies of Ga atoms within the same layer were fixed to 2/3 in the last refinement cycles, whereas their anisotropic thermal parameters were constrained to be equal, in order to limit the number of structural variables. Indeed, the statistical occupation of the cationic sites in a cell with a reduced volume (to which a low density of reflections in the reciprocal space is related) leads to a noticeable increase of the number of parameters needed for describing the structure, reducing the data to variable ratio. Nonetheless the results obtained are highly reliable and the refinement converged with agreement indices R1 = 0.0621 for 65 $F_o > 4\sigma(F_o)$ and R1 = 0.1123 for all 101 data, GOF = 1.077. Crystal data and refined parameters are summarized in Table S1 in the Supporting Information, while relevant bond lengths and the results of bond strength−bond length analysis are reported in Table 1.

The crystal structure is shown in Figure 2 and consists of a 4H stacking of close-packed oxygen layers, in which, similarly to what isobserved in β-Ga_2O_3,[20] both the octahedral and tetrahedral cavities are occupied by gallium ions. Within two adjacent oxygen layers, the cavities are partially occupied, so that the Ga_2O_3 stoichiometry is guaranteed by the presence of Ga vacancies. Two types of layers alternate along the stacking direction: in the first one only the octahedral cavities are occupied (GA1) in a 2/3 ratio, whereas in the second the occupancy of both octahedral (GA2) and tetrahedral (GA3) cavities further complicates the picture.

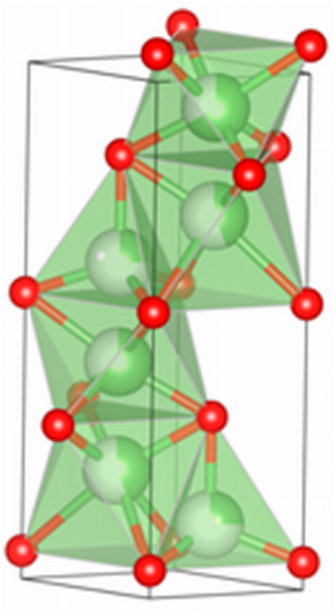

Figure 2. ε-Ga_2O_3 structure representation. Green balls are gallium ions and red balls oxygen atoms.

As discussed before, the independent refinement of GA2 and GA3 occupancies clearly indicates that the two sites are occupied in a mutually exclusive way, which allows maintenance of the stoichiometric cation to oxygen ratio. This situation may derive from a purely stochastic occupation of the gallium sites, although the presence of an ordered superstructure cannot be ruled out. Actually, if the domain size is below the coherence length of the X-rays or the satellite intensities are too low, only an averaged structure can be observed in the diffraction experiment. However, different stacking sequences can reasonably be hypothesized, a few examples of which are reported in Figure 3.

The refined structure is in good agreement with that, ascribed to the Ga_2O_3 ε phase, recently proposed by Playford et al.[15] on the basis of neutron powder diffraction data and pair distribution function analyses of polycrystalline samples including both the β and ε phases. The present study, based on the refinement of single-crystal data, provides new knowledge of ε-Ga_2O_3, adding moreover relevant information about the epitaxial relation with the sapphire substrate, of great relevance for application. On comparison to the well-known and thermodynamically stable β-Ga_2O_3, the average bond distances of the ε phase are in general longer, in agreement with

DOI: 10.1021/acs.inorgchem.6b02244
Inorg. Chem. XXXX, XXX, XXX−XXX

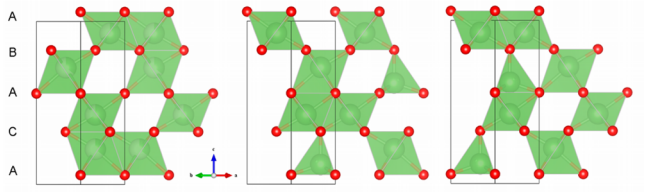

Figure 3. ε-Ga_2O_3 4H structure viewed along the [1−100] direction. The three panels correspond to examples of possible stackings; in each layer 2/3 of the Ga sites are occupied.

vacancy-characterized structures, with the least occupied octahedron showing the longest bonds. The charge distribution analysis, performed with the CHARDIS99 program[21] and making use of bond strength−bond length relations, indicates formal oxidation states of 1.979, 1.011, and 1.01 for the GA1, GA2, and GA3 sites, respectively. Taking into account their partial occupation, one obtains the oxidation states 2.968 for GA1, 2.889 for GA2, and 3.176 for GA3, quite close to the 3+ value expected on the basis of the refined stoichiometry. It is worth noting that, in agreement with the polar character of the space group, the positive and negative charges do not mutually compensate along the z direction, giving rise to nonzero electrical dipoles. Consequently, the phase should be pyroelectric and, on the basis of the structural information, have an electrical polarization of 0.18 $\mu C/cm^2$, as estimated using a simple point-charge model. Additional DHM measurements were carried out in order to assess the actual character of the ε-Ga_2O_3 polymorph, demonstrating that this material is indeed ferroelectric. As mentioned above, we used triangular pulses of 1 kV amplitude for such measurements. In the whole frequency range, the tested sample behaves as a good dielectric material with negligible presence of leakage currents. The registered value of the relative dielectric constant is around 7.17 at 1 kHz (lower than the value of about 8.6 expected for bulk sapphire,[22] measured at 1000 Hz) while the measured resistivity is 1.74×10^{12} Ω cm. Under 1 Hz bias condition, we succeeded in detecting the electrical polarization loop of ε-Ga_2O_3. To do so, raw data had to be elaborated, i.e. by deleting the V-invariant displacement current of sapphire and taking into account the very weak leakage currents. The result of this process is shown in Figure 4. The present measurement, obtained by the integration of the current signal shown in Figure S3 in the Supporting Information, clearly indicates the formation of net

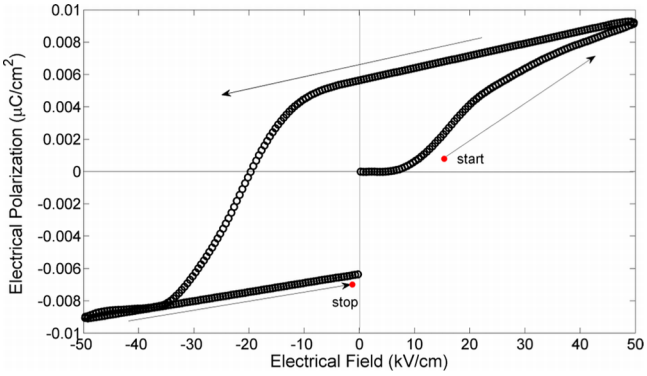

Figure 4. DHM measurement of the electrical polarization performed at room temperature by applying (1 Hz, 1 kV) triangular pulses on a sample constituted by a substrate of sapphire over which ε-Ga_2O_3 was grown.

polarization with maximum value of 0.0092 $\mu C/cm^2$ arising from a depolarized state. The hysteresis characteristic shows that the polarization is not saturated, at least by applying a field up to 50 kV/cm. It is noteworthy that, in the present measurement configuration, the electric field is applied perpendicular to the film surface and is consequently parallel to the polar c-axis of the compound.

Unfortunately, it was not possible to reach the polarization saturation in these ε-Ga_2O_3 films, as dielectric breakdown always occurred at electric fields of about 60 kV/cm in different samples. Hence, just a minor loop is covered in the figure. In any case, by taking the polarization sign change one may determine the coercive field: this was E_C = 20.7 kV/cm for the sample reported in Figure 4. In principle, this consideration may justify the consistent difference between the measured $P_{S,rel}$ and the saturation polarization estimated by calculations on the basis of the structural analysis (e.g., 0.18 $\mu C/cm^2$). The coexistence of semiconducting and ferroelectric properties is an unusual occurrence in solid-state physics and might open the route to the application of this material in new technological fields: for instance, by exploiting the charge separation induced by the internal electrical field. This could help to overcome the well-known limits of oxide semiconductors: i.e. the lack of an effective p-type conductivity. The ferroelectricity of ε-Ga_2O_3, presented here for the first time, makes this compound an interesting playground for additional experimentations.

A precise epitaxial relation is observed in the diffraction images, and this is not surprising if the ε-Ga_2O_3 and Al_2O_3 structures are compared. As shown in Figure 5, sapphire is indeed composed of identical layers of face-sharing AlO_6 octahedra packed with hexagonal symmetry and stacked along the z direction of the lattice.

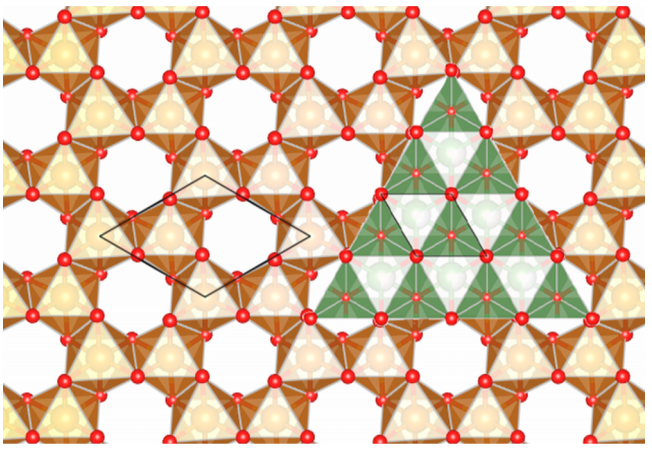

Figure 5. Al_2O_3 (orange) and ε-Ga_2O_3 (green) structures projected along the mutual (0001) direction, highlighting the epitaxial relation between the two lattices.

Two-thirds of the sites are periodically unoccupied in each layer, and the voids are shifted along the (1−100) direction in the z-adjacent layers. As discussed previously, ε-Ga_2O_3 is composed of layers of face-sharing polyhedra: one of the layers is composed solely of the octahedra occupied by the GA1 ion, while the second layer contains both octahedrally (GA2) and tetrahedrally (GA3) coordinated ions. In all cases the distance between adjacent cations atoms in the ab plane is 2.91 Å, while it is 2.79 Å in Al_2O_3, thus revealing a relatively good condition for epitaxy, with a compressive lattice mismatch of about 4.1%.

DOI: 10.1021/acs.inorgchem.6b02244
Inorg. Chem. XXXX, XXX, XXX−XXX

Within this framework, it is easy to understand the partial occupation of the cation sites in ε-Ga_2O_3, with the need to guarantee both the Ga−O stoichiometric ratio and electrical neutrality of the building blocks. Consequently, in strict analogy with Al_2O_3, 2/3 of the sites are occupied on the GA1 layer and the same applies to the GA2/GA3 layer, where the sum of the occupancies is again 2/3. It is interesting to note that in this layer the smaller GA3 tetrahedral site, occupied with 31.8% of probability (i.e., almost 1/3), is likely used to release the compressive strain produced during the epitaxial growth. The present data are not sufficient, alone, to determine the local structure of the Ga_2O_3 film. Actually, the observed fractional occupation could be related to merely statistical occupation of the sites as well as to short-range ordered domains. However, considering that the growth process first involves nucleation on the sapphire substrate, followed by in-plane growth and coalescence,[11] it can be hypothesized that ordered Al_2O_3-like islands with lateral dimensions smaller that the X-ray coherency length initially form, driving the following growth steps. This would be in agreement with the limited strain (or the apparent absence of it) in the deposited Ga_2O_3 film, resulting in well-shaped spherical diffraction spots. Additional high-resolution TEM measurements are in progress to shed some light on the order−disorder question.

CONCLUSIONS

The structural properties of hexagonal ε-Ga_2O_3 deposited on *c*-oriented sapphire by low-temperature MOCVD were thoroughly investigated. The performance of single-crystal X-ray diffraction experiments on a "composite" ε-Ga_2O_3/sapphire sample allowed the accurate determination of the crystal structure of the ε-Ga_2O_3 phase, revealing at the same time a well-defined epitaxial relation with the substrate, the ε-Ga_2O_3 [10−10] direction being parallel to the α-Al_2O_3 [11−20], yielding a lattice mismatch of about 4.1%. Structure solution and refinement were carried out in the polar noncentrosymmetric $P6_3mc$ space group. The structure consists of a 4H stacking of close-packed oxygen layers, in which Ga atoms occupy both octahedral and tetrahedral sites, as in the stable β-phase. Two types of cationic layers are alternatively stacked along the *c* direction, one involving octahedral sites occupied by the gallium ions with a 66% probability, while in the second both octahedral and tetrahedral sites are present, once again with a global occupancy limited to 2/3. This result is in agreement with the expected Ga/O ratio for the Ga_2O_3 composition, while bond strength−bond length calculations confirm the 3+ oxidation state for all of the gallium ions. These findings may be explained by a random occupation of the gallium sites, even if some ordering phenomena (ordered superstructure) are likely. Unfortunately, due to experimental limitations (e.g., small coherence domains, low intensities, Al_2O_3 substrate absorption effects), it is not possible to make a decisive statement here about the order−disorder topic. In addition, the structure refinement showed that the gallium and oxygen ion pattern is such that it gives rise to uncompensated electrical dipoles and indeed the unambiguous ferroelectric hysteresis minor loop was measured by the DHM technique. This is the first time that ferroelectricity has been unambiguously detected in a Ga_2O_3 polymorph. The coexistence of semiconducting and ferroelectric properties is rather unusual and makes this material worthy of further studies, aiming in particular at developing novel application fields.

ASSOCIATED CONTENT

Supporting Information

The Supporting Information is available free of charge on the ACS Publications website at DOI: 10.1021/acs.inorgchem.6b02244.

Reconstructed precession images in 1*kil* projection, complete structural information, ferroelectric measurements details and raw current data obtained from the DHM experiment (PDF)

Crystallographic data (CIF)

AUTHOR INFORMATION

Corresponding Author

*E-mail for F.M.: francesco.mezzadri@unipr.it.

Funding

The Ph.D. scholarship of F. Boschi was provided by Fondazione Cariparma.

Notes

The authors declare no competing financial interest.

ACKNOWLEDGMENTS

The authors are indebted to Prof. M. Solzi for providing access to his FE measurement facilities.

REFERENCES

(1) Villora, E. G.; Shimamura, K.; Yoshikawa, Y.; Aoki, K.; Ichinose, N. Large-size β-Ga_2O_3 single crystals and wafers. *J. Cryst. Growth* **2004**, *270*, 420−426.

(2) Aida, H.; Nishiguchi, K.; Takeda, H.; Aota, N.; Sunakawa, K.; Yaguchi, Y. Growth of β-Ga_2O_3 Single Crystals by the Edge-Defined, Film Fed Growth Method. *J. Appl. Phys.* **2008**, *47*, 8506−8509.

(3) Galazka, Z.; Uecker, R.; Irmscher, K.; Albrecht, M.; Klimm, D.; Pietsch, M.; Brützam, M.; Bertram, R.; Ganschow, S.; Fornari, R. Czochralski growth and characterization of β-Ga_2O_3 single crystals. *Cryst. Res. Technol.* **2010**, *45*, 1229−1236.

(4) Oshima, T.; Arai, N.; Suzuki, N.; Ohira, S.; Fujita, D. Surface morphology of homoepitaxial β-Ga_2O_3 thin films grown by molecular beam epitaxy. *Thin Solid Films* **2008**, *516*, 5768−5771.

(5) Sasaki, K.; Higashiwaki, M.; Kuramata, A.; Masui, T.; Yamakoshi, S. Size control of self-assembled InP/GaInP quantum islands. *J. Cryst. Growth* **2013**, *378*, 591−595.

(6) Wagner, G.; Baldini, M.; Gogova, D.; Schmidbauer, M.; Schewski, R.; Albrecht, M.; Galazka, Z.; Klimm, D.; Fornari, R. Homoepitaxial growth of β-Ga_2O_3 layers by metal-organic vapor phase epitaxy. *Phys. Status Solidi A* **2014**, *211*, 27−33.

(7) Higashiwaki, M.; Sasaki, K.; Kuramata, A.; Masui, T.; Yamakoshi, S. Development of gallium oxide power devices. *Phys. Status Solidi A* **2014**, *211*, 21−26.

(8) Guo, D.; Wu, Z.; Li, P.; An, Y.; Liu, H.; Guo, X.; Yan, H.; Wang, G.; Sun, C.; Li, L.; Tang, W. Fabrication of β-Ga_2O_3 thin films and solar-blind photodetectors by laser MBE technology. *Opt. Mater. Express* **2014**, *4*, 1067−1076.

(9) Roy, R.; Hill, V. G.; Osborn, E. F. Polymorphism of Ga_2O_3 and the system Ga_2O_3-H_2O. *J. Am. Chem. Soc.* **1952**, *74*, 719−722.

(10) Oshima, Y.; Víllora, E. G.; Matsushita, Y.; Yamamoto, S.; Shimamura, K. Epitaxial growth of phase-pure ε-Ga_2O_3 by halide vapor phase epitaxy. *J. Appl. Phys.* **2015**, *118*, 085301−1−5.

(11) Boschi, F.; Bosi, M.; Berzina, T.; Buffagni, E.; Ferrari, C.; Fornari, R. Hetero-epitaxy of ε-Ga_2O_3 layers by MOCVD and ALD. *J. Cryst. Growth* **2016**, *443*, 25−30.

(12) Xia, X.; Chen, Y.; Feng, Q.; Liang, H.; Tao, P.; Xu, M.; Du, G. Hexagonal phase-pure wide band gap ε-Ga_2O_3 films grown on 6H-SiC substrates by metal organic chemical vapor deposition. *Appl. Phys. Lett.* **2016**, *108*, 202103−1−5.

DOI: 10.1021/acs.inorgchem.6b02244
Inorg. Chem. XXXX, XXX, XXX−XXX

(13) Yoshioka, S.; Hayashi, H.; Kuwabara, A.; Oba, F.; Matsunaga, K.; Tanaka, I. Structures and energetics of Ga_2O_3 polymorphs. *J. Phys.: Condens. Matter* **2007**, *19* (11pp), 346211.
(14) Maccioni, M. B.; Fiorentini, V. Phase diagram and polarization of stable phases of $(Ga_{1-x}In_x)_2O_3$. *Appl. Phys. Express* **2016**, *9*, 041102−1−4.
(15) Playford, H. Y.; Hannon, A. C.; Barney, E. R.; Walton, R. I. Structures of Uncharacterised Polymorphs of Gallium Oxide from Total Neutron Diffraction. *Chem. - Eur. J.* **2013**, *19*, 2803−2813.
(16) Baldini, M.; Albrecht, M.; Fiedler, A.; Irmscher, K.; Schewski, R.; Wagner, G. Si- and Sn-Doped Homoepitaxial β-Ga_2O_3 Layers Grown by MOVPE on (010)-Oriented Substrates. *ECS J. Solid State Sci. Technol.* **2017**, *6*, Q3040−Q3044.
(17) Genzel, C. A self-consistent method for X-ray diffraction analysis of multiaxial residual-stress fields in the near-surface region of polycrystalline materials. II. Examples. *J. Appl. Crystallogr.* **1999**, *32*, 779−787.
(18) Burla, M. C.; Caliandro, R.; Camalli, M.; Carrozzini, B.; Cascarano, G. L.; Giacovazzo, C.; Mallamo, M.; Mazzone, A.; Polidori, G.; Spagna, R. SIR2011: a new package for crystal structure determination and refinement. *J. Appl. Crystallogr.* **2012**, *45*, 357−361.
(19) Sheldrick, G. M. Crystal structure refinement with SHELXL. *Acta Crystallogr., Sect. C: Struct. Chem.* **2015**, *71*, 3−8.
(20) Åhman, J.; Svensson, G.; Albertsson, J. A Reinvestigation of β-Gallium Oxide. *Acta Crystallogr., Sect. C: Cryst. Struct. Commun.* **1996**, *52*, 1336−1338.
(21) Nespolo, M.; Ferraris, G.; Ohashi, H. Charge distribution as a tool to investigate structural details: meaning and application to pyroxenes. *Acta Crystallogr., Sect. B: Struct. Sci.* **1999**, *55*, 902−916.
(22) McConnell, R. D.; Wolf, S. *Science and Technology of Thin Film Superconductors*; Springer: Berlin, 1989.

DOI: 10.1021/acs.inorgchem.6b02244
Inorg. Chem. XXXX, XXX, XXX−XXX